

1 **Minimal Influence of Material Surface Properties on Initial Bacterial Attachment to Built**  
2 **Environment Surfaces**

3

4

5 **AUTHOR DETAILS**

6 Kobi Talma<sup>a</sup>, Nathan Bossa<sup>a</sup>, Evan Hankinson<sup>a</sup>, Lijia Gao<sup>a</sup>, Aicha El Kharraf<sup>b</sup>, Mark Wiesner<sup>a\*</sup>

7 <sup>a</sup>Department of Civil and Environmental Engineering, Duke University, Durham, NC, USA

8 <sup>b</sup>Géosciences Rennes, University Rennes, CNRS, UMR 6118, F-, Rennes 35000, France

9 \*Corresponding Author: [Mark Wiesner, [wiesner@duke.edu](mailto:wiesner@duke.edu)]

10

11

12 **ABSTRACT**

13 Biofilms in the built environment (BE) can harbor pathogens and have been linked with  
14 negative health outcomes, particularly in hospital environments. The formation of biofilms  
15 requires bacterial cell attachment on surfaces, such as hospital plumbing, which can have varying  
16 properties, including roughness, wettability, chemistry, and charge. Despite the importance of  
17 bacterial attachment to surfaces, the role of multiple surface properties has been minimally  
18 investigated. Using seven materials with differing surface characteristics, this work considers the  
19 initial attachment of *Escherichia coli*, *Pseudomonas aeruginosa*, *Bacillus subtilis*, and  
20 *Staphylococcus aureus* to investigate the impact of several surface characteristics. Initial  
21 attachment was evaluated using column experiments and compared to batch experiments in which  
22 bacterial growth on coupons was monitored. The attachment of all bacterial species was not  
23 influenced by material surface properties, with similar attachment seen across materials tested.

24 Bacterial cell envelope morphology affected attachment, with gram-negative species displaying  
25 greater attachment than gram-positive species. Attachment efficiency ( $\alpha$ ) was found to be a good  
26 predictor of bacterial attachment, with greater sensitivity than batch tests. Establishment of  
27 commensal communities should be the focus for limiting pathogens in the BE, as engineering  
28 surfaces to reduce microbial attachment appears to offer limited benefit.

29

30

### 31 **KEYWORDS**

32 bacteria, attachment efficiency ( $\alpha$ ), materials, surface properties, cell envelope morphology

33

34

### 35 **INTRODUCTION**

36 Pathogen presence in the built environment (BE) poses a risk to human health. This is  
37 particularly relevant in settings such as hospitals, where hospital-acquired infections represent a  
38 significant burden on the healthcare system. The annual cost of hospital-acquired infections is as  
39 high as \$9.8 billion<sup>1</sup> in the United States healthcare system, and premise plumbing has been shown  
40 to support the growth of pathogenic bacteria and contribute to between 7% and 40% of  
41 infections<sup>2,3</sup>. This pathogen growth often occurs in the form of biofilms, which can serve as a  
42 protective barrier in extreme environments<sup>4</sup>. For example, bacteria established in hospital  
43 plumbing may migrate from these biofilm reservoirs, up towards the sink drain, where droplet  
44 dispersion during faucet operation can lead to infection<sup>5</sup>. The formation of bacterial biofilm  
45 involves several steps: (1) attachment, (2) microcolony formation, (3) matrix formation, (4)  
46 macrocolony formation, also known as maturation, and (5) dispersal<sup>6</sup>. The attachment of bacterial

47 cells to surfaces is therefore an integral step to the establishment and reestablishment of biofilms.  
48 The use of antimicrobial chemicals, including those to coat surfaces, may increase the prevalence  
49 of antimicrobial resistance<sup>7,8</sup>. The current work explores the impacts of surface properties on initial  
50 bacterial attachment, with the possibility of manipulating surface properties to limit bacterial  
51 attachment as a chemical-free strategy for combating biofilm formation without increasing  
52 antimicrobial resistance.

53 Bacterial attachment and biofilm formation have been studied previously in various  
54 contexts, including medical devices<sup>9,10,11</sup>, membrane biofouling<sup>12</sup>, and marine biofouling<sup>13</sup>.  
55 Surface properties play a role in attachment through attractive (van der Waals) and repulsive  
56 (electrostatic) forces. Although numerous studies have investigated the impact of material  
57 properties on bacterial attachment or adhesion, most of these studies have focused on the impact  
58 of a single surface property, and efforts to assess the impact of multiple surface properties are  
59 essential to advance knowledge<sup>14</sup>. Environmental sampling of the BE has largely failed to consider  
60 the impact of any material property on the microbes of the BE, let alone multiple properties<sup>15</sup>. This  
61 further amplifies the need to understand the collective impact of multiple surface properties on  
62 bacterial attachment and the microbiome of the BE.

63 In previous studies, the quantification of bacterial adhesion or attachment has been studied  
64 using batch tests, where bacteria were put in contact with materials for a defined time period, and  
65 cells remaining on the materials' surface after rinsing were quantified. While such an approach  
66 yields useful information concerning the tendency of bacteria to establish themselves on a given  
67 surface, it does not provide kinetic information on the attachment process and is far from real-life  
68 conditions (i.e., fluid dynamics, high contact surfaces, limited nutrients). Alternatively, the concept  
69 of attachment efficiency has been used extensively in colloid science to quantify the affinity of

70 particles for surfaces in a kinetic context, where  $\alpha$  can have values between 0 and 1, and describes  
71 the likelihood of a particle attaching upon interacting with a surface. This approach has been used  
72 for predicting particle removal in water treatment<sup>16,17,18</sup>, bacterial transport in bioremediation<sup>19</sup>,  
73 and the fate and transport of nanomaterials<sup>20,21,22,23</sup>. Surface attachment efficiency,  $\alpha$ , is the ratio  
74 between the number of successful attachments and the number of collisions with the surface and  
75 is typically a function of surface properties (of both the particle and the surface) and environmental  
76 conditions. Combined physical and hydrodynamic models for particle motion,  $\alpha$ , can be used to  
77 determine rates of attachment in porous media<sup>24</sup>. It has also been used to determine aggregation  
78 rates<sup>25</sup>, with applications in natural<sup>26,27</sup> and engineered systems<sup>28</sup>.

79 In this study, we explore the initial attachment of bacteria to relevant, well-characterized  
80 BE materials to fill the gap in assessing multiple surface characteristics' impact on bacterial  
81 attachment. We used model bacteria (*Escherichia coli* K-12 and *Bacillus subtilis* ATCC1174) and  
82 environmentally isolated bacteria (*Pseudomonas aeruginosa* and *Staphylococcus aureus*) to  
83 investigate their attachment to seven BE materials (acrylonitrile butadiene styrene, high-density  
84 polyethylene, high-impact polystyrene, polycarbonate, polyvinyl chloride, polyvinylidene  
85 fluoride, and stainless steel) in representative water chemistry.

86

87

## 88 **MATERIAL AND METHODS**

### 89 **Material Preparation**

90 Pre-production pellets of six polymers: acrylonitrile butadiene styrene (ABS), high-density  
91 polyethylene (HDPE), high-impact polystyrene (HIPS), polycarbonate (PC), polyvinyl chloride  
92 (PVC), and polyvinylidene fluoride (PVDF); and stainless steel (SS) spheres were used in this

93 work. ABS, HDPE, HIPS, PC, and PVDF were purchased from McMaster Carr (Elmhurst,  
94 Illinois). PVC was purchased from Alphagary (Pineville, North Carolina). SS was purchased from  
95 MSE Supplies (Tucson, Arizona). To prepare the materials, 250mL batches of pellets/spheres were  
96 washed in 70% ethanol. After ethanol washing, the pellets/spheres were rinsed thoroughly with  
97 deionized water three times. Pellets/spheres were then air dried in a laminar flow hood and stored  
98 in an autoclaved, airtight container until use.

99

100

## 101 **Material Characterization**

102 The water contact angle (WCA) was measured to determine the surface wettability of the  
103 materials, using the sessile drop method with an optical tensiometer (Attension Theta Flex, Biolin  
104 Scientific; Phoenix, Arizona). Surface roughness was measured by 3D optical/ laser confocal  
105 profilometry (VK-X3000, Keyence; Itasca, Illinois) using a 50x objective, with images  $208\mu\text{m} \times$   
106  $278\mu\text{m}$  collected for each material type. For cylindrical pellets (ABS, HIPS, and PC), images were  
107 taken of both the flat surface (top of cylinder) and the curved surface (lateral surface). The  
108 roughness of cylindrical pellets (ABS, HIPS, and PC) is reported as the weighted average of the  
109 flat and curved surfaces of the materials, assuming the flat surface covers one-third of the total  
110 surface area, and the curved surface covers the other two-thirds of the total surface area. The  
111 surface charge was measured as zeta potential using a solid surface zeta potentiometer (SurPass,  
112 Anton Paar; Austria). The surface charge was measured across a pH range from 2.7 to 7.8, a  
113 Boltzmann curve was fit to the zeta potential data, and the zeta potential at pH 7.5 was determined.  
114 Fourier transform infrared spectrophotometry (FTIR) (Nicolet iS50, ThermoFisher Scientific;  
115 Waltham, Massachusetts) was used to evaluate surface functional groups. Thirty-two scans were

116 performed over the spectral range of 3600-400  $\text{cm}^{-1}$ , and spectra processing was performed using  
117 Spectragryph<sup>29</sup>.

118

119

## 120 **Bacterial Preparation and Characterization**

121 The four model organisms used in this study were *Escherichia coli* K-12 (*E. coli*), an  
122 environmental isolate of *Pseudomonas aeruginosa* (*P. aeruginosa*) from a hospital sink P-trap,  
123 *Bacillus subtilis* ATCC 1174 (*B. subtilis*), and an environmental isolate of *Staphylococcus aureus*  
124 (*S. aureus*) from a hospital sink basin. The model organisms were grown in liquid cultures in  
125 Lennox Luria Broth (LB) media (Sigma-Aldrich; St. Louis, Missouri) to a stationary phase at 37°C  
126 with shaking. After reaching the stationary phase, the liquid cultures were centrifuged in 50mL  
127 tubes at 3000xg and 4°C for 10 minutes. The nutrient media was aspirated from the tubes, and the  
128 pelleted bacteria were resuspended in EPA Moderately Hard water (EPA Mod Hard).

129 Cell surface charge was measured by zeta potential, calculated from electrophoretic  
130 mobility measurements using a Malvern Zetasizer Nano ZS (Malvern; United Kingdom). Cell  
131 hydrophobicity was determined using water contact angle measurements using the sessile drop  
132 method with an optical tensiometer (Attension Theta Flex, Biolin Scientific; Phoenix, Arizona)<sup>30</sup>.

133

134

## 135 **Bacterial Attachment in Dynamic Column Conditions**

136 The column testing setup was modified from Rogers et al.<sup>24</sup> and was organized as follows:  
137 dry pellets/spheres were packed into a glass column (25mm x 150mm, Diba Omnifit EZ  
138 Chromatography Column, Cole Parmer; Vernon Hills, Illinois) to the 11mm line. Deionized water

139 was pumped into the column from the bottom by a syringe pump until the column was filled with  
140 water. The column effluent passed into an in-line ultraviolet-visible spectrophotometer (Evolution  
141 201 UV-visible Spectrophotometer, CAT# 912A0883, ThermoFisher Scientific; Waltham,  
142 Massachusetts). The bacteria sample was passed directly into the spectrophotometer, bypassing  
143 the column by means of T-connectors, to obtain a maximum absorbance at 600nm for the sample  
144 (the initial bacteria concentration,  $C_0$ ). The tubing was flushed with deionized water to remove all  
145 of the bacteria from the system. Then, roughly 3 pore volumes of the background solution (EPA  
146 Mod Hard) were passed through the column to equilibrate the packing material with the  
147 background. The bacteria sample was passed through the column at a flow rate of 2.95mL/min,  
148 and the absorbance was recorded at approximately every 10 seconds for at least 4 pore volumes.

149 A tracer study using potassium nitrate was performed to confirm the integrity of the  
150 column. Column experiments were also carried out using positively charged aminated 1 $\mu$ m silica  
151 particles to calculate  $\alpha$ . The details of the tracer study and positive particle column experiments  
152 are included in the Supporting Information.

153

154

### 155 **Calculation of Attachment Efficiency ( $\alpha$ )**

156 Colloid filtration theory was used to describe bacterial attachment using  $\alpha$ .  $\alpha$  can be  
157 expressed as a function of experimentally observed concentrations of particles in the column  
158 effluent ( $C$ ) and influent ( $C_0$ )<sup>31</sup>:

$$159 \quad \alpha = -\frac{2}{3} \left( \frac{d_c}{(1-\varepsilon)L\eta_0} \right) \ln \frac{C}{C_0} \quad (1)$$

160 where  $d_c$  is the diameter of the collector (pellet/sphere),  $\varepsilon$  is the porosity of the column,  $L$  is the  
161 column length, and  $\eta_0$  is the predicted single-collector contact efficiency.

162 Using the aminated 1 $\mu$ m silica particles as an assumed  $\alpha = 1$  particle, due to their positive  
163 charge, the value of  $\alpha$  was determined using Eq. 2, with the values of  $C/C_0$  taken from the steady-  
164 state phase of the column data. Experiments for  $\alpha$  were conducted in duplicate, and the standard  
165 error is reported to compare between experiments.

$$166 \quad \alpha = \frac{\ln \frac{C}{C_{0bacteria}}}{\ln \frac{C}{C_{0silica}}} * \left( \frac{1}{\frac{L_{bacteria}}{L_{silica}} * \frac{1 - \epsilon_{bacteria}}{1 - \epsilon_{silica}}} \right) \quad (2)$$

167

168

### 169 **Bacterial Attachment in Static Batch Conditions**

170 Batch attachment experiments were carried out as an additional method for determining  
171 the attachment of the model bacteria to the materials tested<sup>32,33</sup>. A known mass of the test material  
172 was incubated with 2mL of the bacterial solution in 5mL glass test tubes at room temperature on  
173 an orbital shaker at 150rpm for 10 minutes. After the incubation period, the bacterial solution was  
174 removed from the test tube, the material was rinsed with 1 $\times$  phosphate-buffered saline (PBS)  
175 (Corning; Manassas, Virginia) three times to remove planktonic bacteria, and the material was  
176 placed into a 15mL centrifuge tube containing 5mL of PBS. Then, the material was vortexed for  
177 1 minute, bath sonicated for 10 minutes, and vortexed for 1 minute to remove attached bacteria.  
178 The removed bacteria were quantified by single plate serial dilution spotting (SP-SDS)<sup>34,35</sup>.

179

180

### 181 **Statistical Analysis**

182 Statistical analysis was conducted for the  $\alpha$  results as a function of material and organism.

183 To test for significance, Kruskal-Wallis and subsequent Dunn's multiple comparisons tests were

184 performed in R for changes in material and organism. The tabulated results of the statistical tests  
185 are included in the Supporting Information.

186

187

## 188 **RESULTS AND DISCUSSION**

### 189 **Characterization of Material Surface Properties**

190 The materials were selected for their range of expected properties and prevalence in the  
191 BE. HDPE and PVC are commonly used for pipe materials, in both distribution systems and  
192 premise plumbing<sup>36</sup>. PVDF is used in high-purity water systems, such as Ultrapure water, due to  
193 its chemical and biological stability<sup>37</sup>. ABS is used in drain-waste-vent systems, which include the  
194 drainpipes from sinks and other plumbing in the BE<sup>38</sup>. HIPS is found in many plastic surfaces in  
195 the BE, particularly in packaging applications<sup>39</sup>. PC is another common plastic material in the BE,  
196 with more resistance than HIPS<sup>40</sup>. SS was selected as a control material and is often used due to  
197 its corrosion-resistant properties<sup>39</sup>.

198 The materials were characterized for several surface properties to identify any differences  
199 that may influence bacterial attachment, and as shown in Table 1, the materials studied presented  
200 different surface properties. The properties that have been the focus of previous studies  
201 investigating bacterial attachment to surfaces are water contact angle<sup>41,42</sup>, roughness<sup>42,43</sup>, and  
202 surface charge<sup>10,44</sup>.

203

204

205

206

207 **Table 1:** Material Properties and Surface Characteristics

<b>Material</b>	<b>WCA<sup>a</sup> (°)</b>	<b>Roughness<sup>a</sup> (nm)</b>	<b>Surface Charge at pH 7.5 (mV)</b>	<b>Surface Functional Groups by FTIR</b>
ABS	92.2 ± 4.5	503.9 ± 160.2	-8.6	C-H; C-H <sub>2</sub> ; C=C; C≡N
HDPE	108.9 ± 2.3	769.0 ± 474.7	-13.2	C-H <sub>2</sub>
HIPS	107.2 ± 6.8	258.2 ± 62.7	-7.9	C-H; C-H=C-H <sub>2</sub> ; C-H; C=C
PC	78.2 ± 2.9	266.0 ± 167.3	-9.8	C-O; C=O; C-H; C-O-C; O-C-O
PVC	89.4 ± 3.7	156.6 ± 37.3	-12.0	C-H; C-H <sub>2</sub> ; C-Cl
PVDF	95.4 ± 4.2	405.4 ± 124.5	-9.1	C-H; C-H <sub>2</sub> ; C-F; C-F <sub>2</sub>
SS	49.9 ± 3.3	50.9 ± 9.9	-18.7	-

208 <sup>a</sup>The error is the standard deviation for all measurement methods.

209

210 Surfaces with water contact angles greater than 90° are generally considered hydrophobic,

211 while those with water contact angles less than 90° are generally regarded as hydrophilic<sup>45</sup>. The

212 selected materials range from hydrophilic (SS) to hydrophobic (HDPE and HIPS), with several

213 materials falling near the 90° threshold. Surface roughness ranged from very smooth (SS = 50.9 ±

214 9.9 nm) to rough (HDPE = 769 ± 474.7 nm). The standard deviation for the roughness

215 measurements describes the heterogeneity of the surfaces, with regions of particularly high

216 roughness visible on some surfaces (Figures S.3.1-S.3.2). The surface charge was negative for all

217 tested materials, ranging between -7.9 mV and -18.7 mV. The surface chemistry was measured

218 using FTIR, and the FTIR spectra are provided in Figure S.6.1 in the Supporting Information. The

219 plastics evaluated in this study (ABS, HDPE, HIPS, PC, PVC, and PVDF) exhibited a range of

220 functional groups, consistent with their polymer composition. ABS, HDPE, and HIPS surfaces

221 showed non-polar groups, with ABS also showing nitrile (C≡N) groups associated with

222 acrylonitrile. PC presents more oxygen-containing surface functionality that makes the surface  
223 more polar, which corresponds with the lower water contact angle than the other plastics. PVC and  
224 PVDF surfaces are chemically distinct, with the presence of chlorine and fluorine on the surface,  
225 respectively. Stainless steel lacks organic functional groups, explaining the lack of signal found  
226 from the FTIR measurement of SS. Interestingly, the material properties measured in this study  
227 showed that while surface charge was similar across materials, the most hydrophilic material (SS)  
228 had the lowest surface roughness, while the material with the greatest roughness (HDPE) was the  
229 most hydrophobic.

230

231

## 232 **Effect of Material Surfaces on Initial Bacterial Attachment**

233 The parameter  $\alpha$  was used to evaluate the initial attachment of bacteria to the selected BE  
234 materials. Two lab-derived bacteria (*E. coli* and *B. subtilis*) and two bacteria isolated from the  
235 hospital environment (*P. aeruginosa* and *S. aureus*) were selected for this study to compare the  
236 initial attachment behavior to bacteria with different cell morphology (Gram-negative vs. Gram-  
237 positive), and different pathogenicity (lab-derived vs. hospital isolates).

238 To determine the value of  $\alpha$  for bacterial cells attaching to BE materials, column  
239 experiments were performed for all four bacterial species using the seven different characterized  
240 materials. Breakthrough curves, where the bacterial cells become observable in the column  
241 effluent, are shown in the Supporting Information. The attachment efficiency to the seven materials  
242 was evaluated for all four bacterial species (*E. coli*, *P. aeruginosa*, *B. subtilis*, and *S. aureus*). The  
243 measured normalized concentrations ( $C/C_0$ ) and calculated  $\alpha$  values are shown in Table 2. For all  
244 materials and bacteria,  $\alpha$  is low with values below 0.02.

245

246 **Table 2:** Calculated Values of  $\alpha$  for Four Bacterial Species to Various Materials

<b>Bacteria</b>	<b>Material</b>	<b><math>C/C_0^a</math></b>	<b><math>\alpha^{a,b}</math></b>
<i>E. coli</i>	ABS	$0.84 \pm 0.054$	$0.018 \pm 0.0066$
	HDPE	$0.86 \pm 0.046$	$0.016 \pm 0.0055$
	HIPS	$0.83 \pm 0.027$	$0.015 \pm 0.0022$
	PC	$0.87 \pm 0.039$	$0.015 \pm 0.0054$
	PVC	$0.86 \pm 0.023$	$0.014 \pm 0.0026$
	PVDF	$0.88 \pm 0.041$	$0.019 \pm 0.0067$
	SS	$0.91 \pm 0.014$	$0.012 \pm 0.0021$
<i>P. aeruginosa</i>	ABS	$0.84 \pm 0.0074$	$0.017 \pm 0.0015$
	HDPE	$0.86 \pm 0.0038$	$0.016 \pm 0.00087$
	HIPS	$0.84 \pm 0.0030$	$0.014 \pm 0.00042$
	PC	$0.87 \pm 0.0034$	$0.015 \pm 0.00013$
	PVC	$0.86 \pm 0.040$	$0.014 \pm 0.0043$
	PVDF	$0.90 \pm 0.0045$	$0.015 \pm 0.00062$
	SS	$0.87 \pm 0.0071$	$0.019 \pm 0.0011$
<i>B. subtilis</i>	ABS	$0.98 \pm 0.014$	$0.0016 \pm 0.0014$
	HDPE	$0.97 \pm 0.013$	$0.0031 \pm 0.0012$
	HIPS	$1.00 \pm 0.0016$	$0.00012 \pm 0.00012$
	PC	$0.98 \pm 0.017$	$0.0019 \pm 0.0019$
	PVC	$0.99 \pm 0.00056$	$0.0012 \pm 0.000087$
	PVDF	$0.94 \pm 0.037$	$0.0089 \pm 0.0053$
	SS	$1.00 \pm 0.0033$	$0.00045 \pm 0.00045$
<i>S. aureus</i>	ABS	$0.96 \pm 0.0024$	$0.0043 \pm 0.00024$
	HDPE	$0.95 \pm 0.0011$	$0.0051 \pm 0.000078$
	HIPS	$0.97 \pm 0.0051$	$0.0026 \pm 0.00046$
	PC	$0.93 \pm 0.031$	$0.0089 \pm 0.003$
	PVC	$0.96 \pm 0.0046$	$0.0041 \pm 0.00051$
	PVDF	$0.93 \pm 0.018$	$0.0099 \pm 0.0027$
	SS	$0.95 \pm 0.0083$	$0.0071 \pm 0.0012$

247 <sup>a</sup>The error is the standard error based on duplicate measurements. <sup>b</sup> $\alpha$  values were compared for  
 248 columns of the same bacterial species.

249           The low attachment found during this study can be explained by repulsive electrostatic  
250 forces between negatively charged surfaces and negatively charged bacterial cells<sup>46,47</sup>. Column  
251 experiments and attachment efficiency ( $\alpha$ ) have been used previously to evaluate the transport and  
252 attachment of bacteria in porous media<sup>48,49,50</sup>, and these studies have found higher attachment than  
253 this study. McCaulou et al. found  $\alpha$  values between 0.04 and 0.4 for the interaction between  
254 bacteria and different quartz surfaces<sup>48</sup>. The largest  $\alpha$  values found were between negatively  
255 charged bacteria and coated surfaces with a positive charge. Deshpande et al. showed that *P.*  
256 *fluorescens* had an  $\alpha$  value of 0.094 when interacting with silica surfaces<sup>49</sup>. Increased ionic strength  
257 increased the attachment of *P. fluorescens*, up to 0.206 at ionic strength of  $3 \times 10^{-2}$ M, which has  
258 also been seen with attachment of other biological particles<sup>24,50</sup>.

259           Usually, hydrophilic surfaces, with increased wettability, led to increased attachment in  
260 previous studies. Bruzaud et al. found that more wild-type *P. aeruginosa* cells attached to a  
261 stainless steel surface with WCA of  $61^\circ$  (attached cells  $\cong 9 \times 10^4$  CFU/cm<sup>2</sup>) than to a  
262 superhydrophobic stainless steel with WCA of  $147^\circ$  (attached cells  $\cong 3 \times 10^3$  CFU/cm<sup>2</sup>)<sup>41</sup>.  
263 Similarly, Liu et al. found increased attachment of *E. coli* on hydrophilic titanium (WCA =  $42.0^\circ$ )  
264 and stainless steel (WCA =  $65.8^\circ$ ) surfaces, compared to hydrophobic Ni-P-PFTE surfaces (WCA  
265  $108.0^\circ$  and  $117.8^\circ$ )<sup>51</sup>. Conversely, another study found that the near-wall velocity of bacteria was  
266 reduced when interacting with hydrophobic surfaces, promoting adhesion to the surface<sup>52</sup>. Rough  
267 surfaces have also been shown to lead to increased microbial attachment. Mu et al. showed that  
268 bacterial densities were low on smooth surfaces, with values between  $2\text{-}3 \times 10^{-2}$  cells/ $\mu\text{m}^2$ , but as  
269 roughness increased, bacterial density increased to  $5\text{-}10 \times 10^{-2}$  cells/ $\mu\text{m}^2$ <sup>42</sup>. Bohnic et al. found  
270 that for surfaces with roughness ranging from  $0.07\mu\text{m}$  to  $5.8\mu\text{m}$ , attachment of bacteria, measured  
271 as crystal violet (CV) absorbance, increased<sup>43</sup>. For *E. coli*, CV absorbance increased from 0.0267

272  $\pm 0.024$  to  $0.3117 \pm 0.054$ . This trend was also seen for *P. aeruginosa* and *S. aureus*, with increases  
273 from  $0.0517 \pm 0.072$  to  $0.9417 \pm 0.11$ , and  $0.0537 \pm 0.019$  to  $0.2697 \pm 0.068$ , respectively. Yang  
274 et al. found a positive correlation between bacterial attachment and surface roughness above a  
275 threshold of  $6 \text{ nm}^{53}$ . However, according to Kruskal-Wallis tests, none of the  $\alpha$  values were  
276 significantly affected by changes in material (Tables S.4.1-4.5.8). Additionally, when bacterial  
277 attachment is plotted against the surface properties of the material, no trend is observed. The results  
278 showed that material properties in this study did not significantly impact initial bacterial  
279 attachment, contrary to previous studies.

280

281

## 282 **Effect of Bacterial Cell Properties on Initial Attachment**

283 The cell surface charge and hydrophobicity of the four bacterial species were measured,  
284 and the results are shown in Table 3, along with the cell envelope morphology and pathogenicity.

285

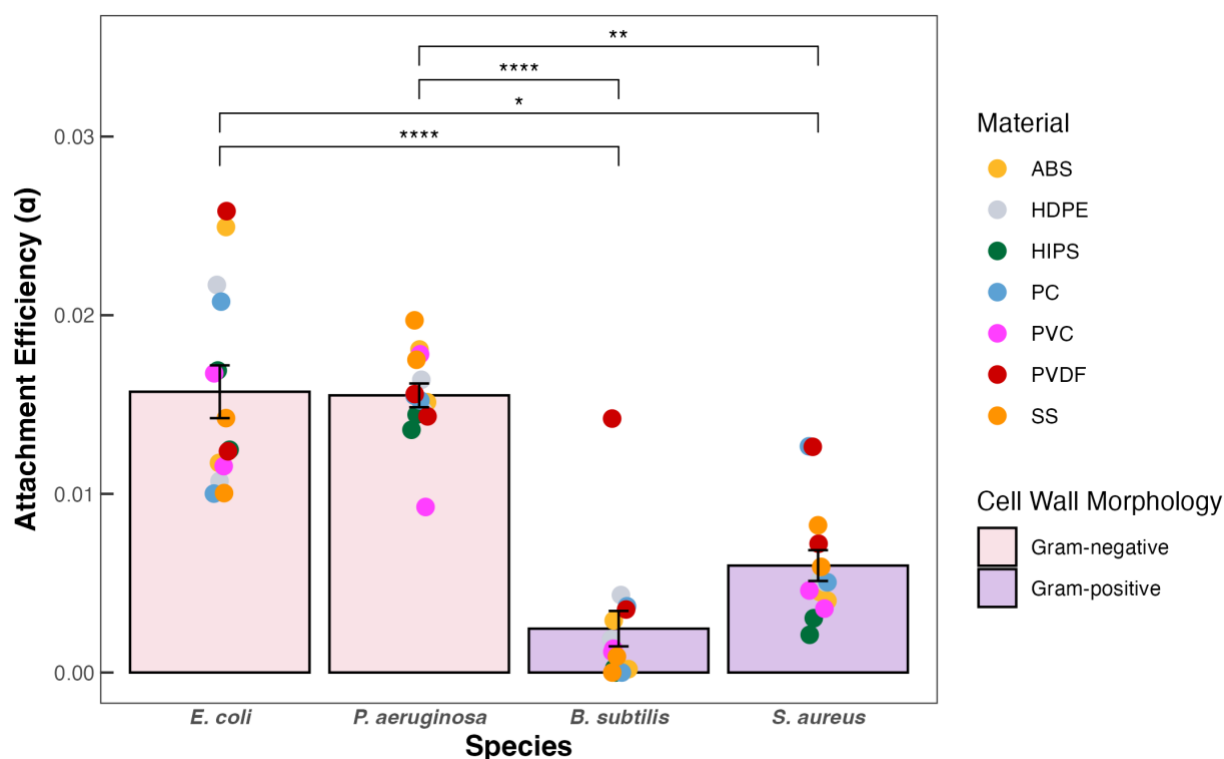
286 **Table 3:** Bacterial Cell Surface Characteristics and Pathogenicity

Species	Cell Surface	Contact angle	Cell Envelope	
	Charge <sup>a,b</sup> (mV)	(Hydrophobicity) <sup>b</sup> (°)	Morphology	Pathogenic
<i>E. coli</i>	$-30.12 \pm 0.56$	$16.85 \pm 1.67$	Gram –	No
<i>P. aeruginosa</i>	$-9.60 \pm 0.50$	$38.28 \pm 6.72$	Gram –	Yes
<i>B. subtilis</i>	$-31.74 \pm 0.35$	$29.57 \pm 1.17$	Gram +	No
<i>S. aureus</i>	$-21.37 \pm 0.38$	$17.97 \pm 0.59$	Gram +	Yes

287 <sup>a</sup>Cell surface charge measured as zeta potential. <sup>b</sup>The error is the standard deviation for all  
288 measurement methods.

289

290 Figure 1 shows the results for  $\alpha$  compared between bacterial species when pooled across all seven  
291 materials. There are statistically significant differences in  $\alpha$  between both Gram-negative species  
292 (*E. coli* and *P. aeruginosa*) and both Gram-positive species (*B. subtilis* and *S. aureus*). The  $\alpha$  results  
293 did not show a dependence on any of the other bacterial cell properties (surface charge,  
294 hydrophobicity, pathogenicity). The initial attachment efficiency of the Gram-negative species  
295 was found to be higher than the initial attachment efficiency of the Gram-positive species by an  
296 order of magnitude (0.016 and 0.016 compared to 0.0025 and 0.0060).  
297



298  
299 **Figure 1:** Average bacterial attachment efficiencies for different bacterial species across all  
300 materials tested. The error bars are the standard error for 14 measurements.

301  
302 Gram-positive bacteria have a thick peptidoglycan layer that increases the rigidity of their  
303 cell envelope<sup>54</sup>. This rigidity may limit initial attachment due to an inability of the cell envelope

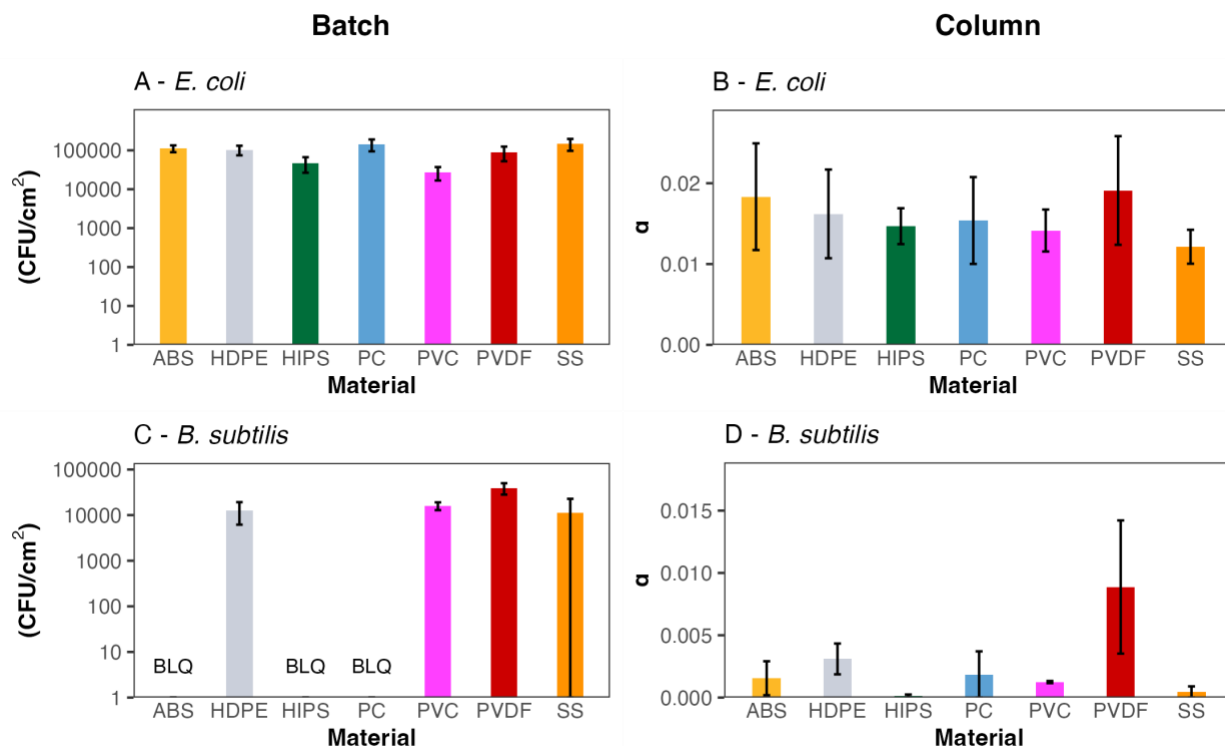
304 to adapt to nanoscale roughness present on the surface, leading to sub-optimal surface contact. The  
305 rigid peptidoglycan layer of Gram-positive bacteria limits mechano-selectivity towards a surface,  
306 compared to the more sensitive surface structures of Gram-negative bacteria<sup>55</sup>. The effect of cell  
307 envelope rigidity was also shown in a study comparing the effect of zero-valent iron, where the  
308 envelope of Gram-negative bacteria was more susceptible to the zero-valent iron adhering to the  
309 cell membrane than that of Gram-positive bacteria<sup>56</sup>. Additionally, Gram-negative bacteria have  
310 external lipopolysaccharides and adhesin proteins on their cell walls, which facilitate attachment  
311 to surfaces<sup>57</sup>.

312

313

#### 314 **Comparing Batch and Column Experimental Approaches for Measuring Bacterial** 315 **Attachment to Surfaces**

316 Column experiments have been utilized to evaluate the transport and attachment of bacteria  
317 in porous media<sup>48,49,50</sup>, but not, to our knowledge, to assess attachment to BE materials. The  
318 attachment of *E. coli* and *B. subtilis* was evaluated using batch tests and compared to attachment  
319 determined using column experiments. Comparing these two methods allowed us to place our  
320 results in context with previous approaches and assess the suitability of column experiments for  
321 determining initial attachment in the BE.



322  
323 **Figure 2:** Attachment results from batch experiments (left panels) and column experiments (right  
324 panels). Panels A and B are results for *E. coli*, and Panels C and D are results for *B. subtilis*. The  
325 error bars for the batch experiment are the standard error for triplicate measurements. The error  
326 bars for the column experiment are the standard error for duplicate measurements. BLQ - below  
327 the limit of quantification, defined as 6 colonies for the SP-SDS method<sup>34,35</sup>.

328  
329 The results of attachment from batch experiments are similar to the results found by the  
330 column experiments when comparing attachment across the tested materials (Figure 2). No  
331 statistical difference in attachment was found between materials for both experimental  
332 methodologies, for both *E. coli* and *B. subtilis*. Interestingly, the column experiments had a higher  
333 sensitivity and were able to determine the attachment efficiency of *B. subtilis* for all seven  
334 materials, while the batch experiments were below the limit of quantification for three materials.  
335 Although the batch and column experiments had similar contact time between material and

336 bacteria, 10 minutes and approximately 7 minutes, respectively, the batch experiments involved  
337 no flow. Furthermore, the batch experiments involved a limited surface area for bacteria-surface  
338 interactions ( $1.19 \pm 0.551 \text{ cm}^2$ ) compared to the column experiments ( $766 \pm 188 \text{ cm}^2$ ). These  
339 factors, along with the real-time monitoring provided by the in-line spectrophotometer, are  
340 hypothesized to be reasons for increased sensitivity of the column experiments when compared to  
341 the batch tests. Previous batch tests have found similar numbers of attached cells compared to this  
342 study. Results for *B. subtilis* showed  $\sim 5.1 \times 10^4 \text{ CFU/cm}^2$  and  $\sim 4.6 \times 10^4 \text{ CFU/cm}^2$  attached to PE  
343 and PVC, respectively<sup>32</sup>. However, results for *E. coli* were lower than those for *B. subtilis*,  
344 contradicting the trend found in this study.

345         The comparison between column experiments and batch experiments, shown in Figure 2,  
346 indicates that column experiments and the calculation of attachment efficiency are an effective  
347 method for testing bacterial attachment to BE materials. An additional advantage of the column  
348 experiments is the ability to test attachment under flow conditions, which is particularly important  
349 for aqueous systems with flow, as it has been shown that adhesion is strengthened by shear stress<sup>58</sup>.  
350 Utilizing column experiments to evaluate bacterial attachment has its advantages but also  
351 limitations. Materials to be tested in this system must fit into a small diameter column to provide  
352 a high surface area to volume ratio, which may limit the variety of materials available for testing.  
353 Additionally, calculating  $\alpha$  assumes a spherical collector material<sup>59</sup>— in our study, plastic pellets or  
354 stainless steel – further limiting the selection of materials upon which bacterial attachment can be  
355 evaluated using this methodology.

356

357

358

## 359 CONCLUSION

360 Overall, these results suggest that initial bacterial attachment to BE materials is uniformly  
361 low, with little to no dependence on any of the physico-chemical properties of the surfaces as  
362 characterized in this work. The initial kinetics of bacterial attachment appear to be much more  
363 dependent on the nature of the cell envelope (morphology, gram-negative vs. gram-positive).  
364 Column experiments and determination of attachment efficiency ( $\alpha$ ) can be an effective method to  
365 compare initial attachment across different bacterial species, particularly when the impact of fluid  
366 flow is relevant. Manipulating material properties to limit initial bacterial attachment may not be  
367 an effective strategy for reducing biofilm formation and the presence of bacterial pathogens due  
368 to the limited differences in material seen in this study. Future directions for limiting bacterial  
369 pathogen presence in the BE should focus on the establishment of beneficial bacterial  
370 communities, along with the effect of material properties on biofilm formation and cleaning  
371 efficiency.

372

373

## 374 ACKNOWLEDGEMENTS

375 We thank Claudia Gunsch and her laboratory (Duke) for providing the *E. coli* and *B.*  
376 *subtilis* strains, and Deverick Anderson and his laboratory (Duke) for providing the *P. aeruginosa*  
377 and *S. aureus* strains. This work was performed in part at the Duke University Shared Materials  
378 Instrumentation Facility (SMIF), a member of the North Carolina Research Triangle  
379 Nanotechnology Network (RTNN), which is supported by the National Science Foundation (award  
380 number ECCS-2025064) as part of the National Nanotechnology Coordinated Infrastructure  
381 (NNCI).

382

383

## 384 **AUTHOR CONTRIBUTIONS**

385           CRedit: **Kobi Talma:** Conceptualization, Formal analysis, Investigation, Methodology,  
386 Visualization, Writing – original draft, Writing – review & editing; **Nathan Bossa:**  
387 Conceptualization, Methodology, Supervision, Writing – review & editing; **Evan Hankinson:**  
388 Investigation; **Lijia Gao:** Visualization, Writing – review & editing; **Aicha El Kharraf:**  
389 Investigation, Writing – review & editing; **Mark Wiesner:** Conceptualization, Funding  
390 acquisition, Supervision, Writing – review & editing.

391

392

## 393 **DISCLOSURE STATEMENT**

394           The authors declare no competing financial interest.

395

396

## 397 **FUNDING STATEMENT**

398           This work was supported primarily by the Engineering Research Centers Program of the  
399 National Science Foundation under NSF Cooperative Agreement No. EEC-2133504.

400

401

## 402 **DATA AVAILABILITY STATEMENT**

403           The data that support the findings of this study are available from the corresponding author  
404 upon reasonable request.

405 **REFERENCES**

- 406 (1) Zimlichman, E.; Henderson, D.; Tamir, O.; Franz, C.; Song, P.; Yamin, C. K.; Keohane, C.;  
407 Denham, C. R.; Bates, D. W. Health Care–Associated Infections. *JAMA Internal Medicine* **2013**,  
408 *173* (22), 2039. DOI: 10.1001/jamainternmed.2013.9763.
- 409 (2) Volling, C.; Mataseje, L.; Graña-Miraglia, L.; Hu, X.; Anceva-Sami, S.; Coleman, B. L.;  
410 Downing, M.; Hota, S.; Jamal, A. J.; Johnstone, J.; et al. Epidemiology of healthcare-associated  
411 *Pseudomonas aeruginosa* in intensive care units: are sink drains to blame? *Journal of Hospital*  
412 *Infection* **2024**, *148*, 77-86. DOI: 10.1016/j.jhin.2024.03.009.
- 413 (3) Regev-Yochay, G.; Margalit, I.; Smollan, G.; Rapaport, R.; Tal, I.; Hanage, W. P.; Pinas  
414 Zade, N.; Jaber, H.; Taylor, B. P.; Che, Y.; et al. Sink-traps are a major source for  
415 carbapenemase-producing *Enterobacteriaceae* transmission. *Infection Control & Hospital*  
416 *Epidemiology* **2024**, *45* (3), 284-291. DOI: 10.1017/ice.2023.270.
- 417 (4) Yin, W.; Wang, Y.; Liu, L.; He, J. Biofilms: The Microbial “Protective Clothing” in Extreme  
418 Environments. *International Journal of Molecular Sciences* **2019**, *20* (14), 3423. DOI:  
419 10.3390/ijms20143423.
- 420 (5) Kotay, S.; Chai, W.; Guilford, W.; Barry, K.; Mathers, A. J. Spread from the Sink to the  
421 Patient: *In Situ* Study Using Green Fluorescent Protein (GFP)-Expressing *Escherichia coli* To  
422 Model Bacterial Dispersion from Hand-Washing Sink-Trap Reservoirs. *Applied and*  
423 *Environmental Microbiology* **2017**, *83* (8), AEM.03327-03316. DOI: 10.1128/aem.03327-16.
- 424 (6) Pal, M.; M N, L. Microbial Influenced Corrosion: Understanding Bioadhesion and Biofilm  
425 Formation. *Journal of Bio- and Tribo-Corrosion* **2022**, *8*. DOI: 10.1007/s40735-022-00677-x.

- 426 (7) Ben Maamar, S.; Hu, J.; Hartmann, E. M. Implications of indoor microbial ecology and  
427 evolution on antibiotic resistance. *Journal of Exposure Science & Environmental*  
428 *Epidemiology* **2020**, *30* (1), 1-15. DOI: 10.1038/s41370-019-0171-0.
- 429 (8) Mäki, A.; Salonen, N.; Kivisaari, M.; Ahonen, M.; Latva, M. Microbiota shaping and  
430 bioburden monitoring of indoor antimicrobial surfaces. *Frontiers in Built Environment* **2023**, *9*.  
431 DOI: 10.3389/fbuil.2023.1063804.
- 432 (9) Busscher, H. J.; Rinastiti, M.; Siswomihardjo, W.; van der Mei, H. C. Biofilm Formation on  
433 Dental Restorative and Implant Materials. *Journal of Dental Research* **2010**, *89* (7), 657-665.  
434 DOI: 10.1177/0022034510368644.
- 435 (10) Gottenbos, B.; Van Der Mei, H. C.; Busscher, H. J.; Grijpma, D. W.; Feijen, J. Initial  
436 adhesion and surface growth of *Pseudomonas aeruginosa* on negatively and positively charged  
437 poly(methacrylates). *Journal of Materials Science: Materials in Medicine* **1999**, *10* (12), 853-  
438 855. DOI: 10.1023/a:1008989416939.
- 439 (11) Loo, C.-Y.; Young, P. M.; Lee, W.-H.; Cavaliere, R.; Whitchurch, C. B.; Rohanizadeh, R.  
440 Superhydrophobic, nanotextured polyvinyl chloride films for delaying *Pseudomonas aeruginosa*  
441 attachment to intubation tubes and medical plastics. *Acta Biomaterialia* **2012**, *8* (5), 1881-1890.  
442 DOI: 10.1016/j.actbio.2012.01.015.
- 443 (12) Alsawaftah, N.; Abuwatfa, W.; Darwish, N.; Husseini, G. A. A Review on Membrane  
444 Biofouling: Prediction, Characterization, and Mitigation. *Membranes* **2022**, *12* (12), 1271. DOI:  
445 10.3390/membranes12121271.
- 446 (13) Dang, H.; Lovell, C. R. Microbial Surface Colonization and Biofilm Development in  
447 Marine Environments. *Microbiology and Molecular Biology Reviews* **2016**, *80* (1), 91-138. DOI:  
448 10.1128/mmbr.00037-15.

- 449 (14) Zheng, S.; Bawazir, M.; Dhall, A.; Kim, H.-E.; He, L.; Heo, J.; Hwang, G. Implication of  
450 Surface Properties, Bacterial Motility, and Hydrodynamic Conditions on Bacterial Surface  
451 Sensing and Their Initial Adhesion. *Frontiers in Bioengineering and Biotechnology* **2021**, *9*.  
452 DOI: 10.3389/fbioe.2021.643722.
- 453 (15) Talma, K.; Sipe, J. M.; Bossa, N.; Stiffler, W.; Hankinson, E.; Gunsch, C.; Wiesner, M.  
454 Material Matters: A Framework for Integrating Surface Properties into Built Environment  
455 Microbiome Research. *Applied and Environmental Microbiology* **In Press**.
- 456 (16) O'Melia, C. R. ES&T Features: Aquasols: the behavior of small particles in aquatic systems.  
457 *Environmental Science & Technology* **1980**, *14* (9), 1052-1060. DOI: 10.1021/es60169a601.
- 458 (17) O'Melia, C. R. Particle-particle interactions. *IN: Aquatic Surface Chemistry: Chemical*  
459 *Processes at the Particle-Water Interface. John Wiley and Sons, New York. 1987. p 385-403, 4*  
460 *fig, 47 ref. NSF Grant 1987*.
- 461 (18) O'Melia, C. R. Particle—particle interactions in aquatic systems. *Colloids and Surfaces*  
462 **1989**, *39* (1), 255-271. DOI: 10.1016/0166-6622(89)80191-x.
- 463 (19) Marlow, H. J.; Duston, K. L.; Wiesner, M. R.; Tomson, M. B.; Wilson, J. T.; Ward, C. H.  
464 Microbial transport through porous media: The effects of hydraulic conductivity and injection  
465 velocity. *Journal of Hazardous Materials* **1991**, *28* (1-2), 65-74. DOI: 10.1016/0304-  
466 3894(91)87006-n.
- 467 (20) Petosa, A. R.; Jaisi, D. P.; Quevedo, I. R.; Elimelech, M.; Tufenkji, N. Aggregation and  
468 Deposition of Engineered Nanomaterials in Aquatic Environments: Role of Physicochemical  
469 Interactions. *Environmental Science & Technology* **2010**, *44* (17), 6532-6549. DOI:  
470 10.1021/es100598h.

- 471 (21) Bossa, N.; Carpenter, A. W.; Kumar, N.; De Lannoy, C.-F.; Wiesner, M. Cellulose  
472 nanocrystal zero-valent iron nanocomposites for groundwater remediation. *Environmental*  
473 *Science: Nano* **2017**, *4* (6), 1294-1303. DOI: 10.1039/c6en00572a.
- 474 (22) Geitner, N. K.; O'Brien, N. J.; Turner, A. A.; Cummins, E. J.; Wiesner, M. R. Measuring  
475 Nanoparticle Attachment Efficiency in Complex Systems. *Environmental Science & Technology*  
476 **2017**, *51* (22), 13288-13294. DOI: 10.1021/acs.est.7b04612.
- 477 (23) Su, Y.; Zhao, Y. S.; Li, L. L.; Qin, C. Y.; Wu, F.; Geng, N. N.; Lei, J. S. Transport  
478 characteristics of nanoscale zero-valent iron carried by three different “vehicles” in porous  
479 media. *Journal of Environmental Science and Health, Part A* **2014**, *49* (14), 1639-1652. DOI:  
480 10.1080/10934529.2014.951214.
- 481 (24) Rogers, N. M. K.; Hicks, E.; Kan, C.; Martin, E.; Gao, L.; Limso, C.; Hendren, C. O.;  
482 Kuehn, M.; Wiesner, M. R. Characterizing the Transport and Surface Affinity of Extracellular  
483 Vesicles Isolated from Yeast and Bacteria in Well-Characterized Porous Media. *Environmental*  
484 *Science & Technology* **2023**, *57* (35), 13182-13192. DOI: 10.1021/acs.est.3c03700.
- 485 (25) Abdolapur Monikh, F.; Quik, J. T. K.; Wiesner, M. R.; Tapparo, A.; Pastore, P.; Grossart,  
486 H.-P.; Akkanen, J.; Kortet, R.; Kukkonen, J. V. K. Importance of Attachment Efficiency in  
487 Determining the Fate of PS and PVC Nanoplastic Heteroaggregation with Natural Colloids  
488 Using a Multimedia Model. *Environmental Science & Technology* **2025**, *59* (9), 4674-4683.  
489 DOI: 10.1021/acs.est.4c10918.
- 490 (26) Pirade, F.; Foppen, J. W.; Van Der Hoek, J. P.; Lompe, K. M. Polystyrene nanoplastics are  
491 unlikely to aggregate in freshwater bodies. *Environmental Pollution* **2025**, *366*, 125393. DOI:  
492 10.1016/j.envpol.2024.125393.

- 493 (27) Geitner, N. K.; Cooper, J. L.; Avellan, A.; Castellon, B. T.; Perrotta, B. G.; Bossa, N.;  
494 Simonin, M.; Anderson, S. M.; Inoue, S.; Hochella, M. F.; et al. Size-Based Differential  
495 Transport, Uptake, and Mass Distribution of Ceria (CeO<sub>2</sub>) Nanoparticles in Wetland Mesocosms.  
496 *Environmental Science & Technology* **2018**, *52* (17), 9768-9776. DOI: 10.1021/acs.est.8b02040.
- 497 (28) Kaegi, R.; Voegelin, A.; Ort, C.; Sinnet, B.; Thalmann, B.; Krismer, J.; Hagendorfer, H.;  
498 Elumelu, M.; Mueller, E. Fate and transformation of silver nanoparticles in urban wastewater  
499 systems. *Water Research* **2013**, *47* (12), 3866-3877. DOI: 10.1016/j.watres.2012.11.060.
- 500 (29) Menges, F. Spectragryph - optical spectroscopy software, Version 1.2.16.1.  
501 <http://www.ffmpeg2.de/spectragryph/>, 2022.
- 502 (30) Busscher, H. J.; Weerkamp, A. H.; Van Der Mei, H. C.; Van Pelt, A. W.; De Jong, H. P.;  
503 Arends, J. Measurement of the surface free energy of bacterial cell surfaces and its relevance for  
504 adhesion. *Applied and Environmental Microbiology* **1984**, *48* (5), 980-983. DOI:  
505 10.1128/aem.48.5.980-983.1984.
- 506 (31) Tufenkji, N.; Elimelech, M. Correlation Equation for Predicting Single-Collector Efficiency  
507 in Physicochemical Filtration in Saturated Porous Media. *Environmental Science & Technology*  
508 **2004**, *38* (2), 529-536. DOI: 10.1021/es034049r.
- 509 (32) Cai, L.; Wu, D.; Xia, J.; Shi, H.; Kim, H. Influence of physicochemical surface properties  
510 on the adhesion of bacteria onto four types of plastics. *Science of The Total Environment* **2019**,  
511 *671*, 1101-1107. DOI: 10.1016/j.scitotenv.2019.03.434.
- 512 (33) Simões, L. C.; Simões, M.; Oliveira, R.; Vieira, M. J. Potential of the adhesion of bacteria  
513 isolated from drinking water to materials. *Journal of Basic Microbiology* **2007**, *47* (2), 174-183.  
514 DOI: 10.1002/jobm.200610224.

- 515 (34) Sieuwerts, S.; De Bok, F. A. M.; Mols, E.; De Vos, W. M.; Van Hylckama Vlieg, J. E. T. A  
516 simple and fast method for determining colony forming units. *Letters in Applied Microbiology*  
517 **2008**, 47 (4), 275-278. DOI: 10.1111/j.1472-765x.2008.02417.x.
- 518 (35) Thomas, P.; Sekhar, A. C.; Upreti, R.; Mujawar, M. M.; Pasha, S. S. Optimization of single  
519 plate-serial dilution spotting (SP-SDS) with sample anchoring as an assured method for bacterial  
520 and yeast cfu enumeration and single colony isolation from diverse samples. *Biotechnology*  
521 *Reports* **2015**, 8, 45-55. DOI: 10.1016/j.btre.2015.08.003.
- 522 (36) Heim, T. H.; Dietrich, A. M. Sensory aspects and water quality impacts of chlorinated and  
523 chloraminated drinking water in contact with HDPE and cPVC pipe. *Water Research* **2007**, 41  
524 (4), 757-764. DOI: 10.1016/j.watres.2006.11.028.
- 525 (37) Park, H.; Kim, S.; Choi, S.; Park, J.; Lee, K.-H.; Kang, S. Comparative Evaluation of PVC  
526 and PVDF Pipe Leaching in Ultrapure Water (UPW) Using Batch and Loop Pilot Systems.  
527 *KSCE Journal of Civil Engineering* **2025**, 100366. DOI: 10.1016/j.kscej.2025.100366.
- 528 (38) PPFa. *ABS SPECIFICATION SHEET: Acrylonitrile Butadiene Styrene (ABS) Plastic Pipe*  
529 *and Fittings for Drainage, Waste and Vent Systems*. 2024.  
530 [https://www.ppfahome.org/resource/resmgr/pdf/PPFA-04-24\\_absspec\\_final\\_pub.pdf](https://www.ppfahome.org/resource/resmgr/pdf/PPFA-04-24_absspec_final_pub.pdf) (accessed  
531 2025 October 28).
- 532 (39) Guazzotti, V.; Gruner, A.; Juric, M.; Hendrich, V.; Störmer, A.; Welle, F. Migration Testing  
533 of GPPS and HIPS Polymers: Swelling Effect Caused by Food Simulants Compared to Real  
534 Foods. *Molecules* **2022**, 27 (3), 823. DOI: 10.3390/molecules27030823.
- 535 (40) Sipe, J. M.; Bossa, N.; Berger, W.; Von Windheim, N.; Gall, K.; Wiesner, M. R. From  
536 bottle to microplastics: Can we estimate how our plastic products are breaking down? *Science of*  
537 *The Total Environment* **2022**, 814, 152460. DOI: 10.1016/j.scitotenv.2021.152460.

- 538 (41) Bruzaud, J.; Tarrade, J.; Coudreuse, A.; Canette, A.; Herry, J.-M.; Taffin de Givenchy, E.;  
539 Darmanin, T.; Guittard, F.; Guilbaud, M.; Bellon-Fontaine, M.-N. Flagella but not type IV pili  
540 are involved in the initial adhesion of *Pseudomonas aeruginosa* PAO1 to hydrophobic or  
541 superhydrophobic surfaces. *Colloids and Surfaces B: Biointerfaces* **2015**, *131*, 59-66. DOI:  
542 10.1016/j.colsurfb.2015.04.036.
- 543 (42) Mu, M.; Liu, S.; Deflorio, W.; Hao, L.; Wang, X.; Salazar, K. S.; Taylor, M.; Castillo, A.;  
544 Cisneros-Zevallos, L.; Oh, J. K.; et al. Influence of Surface Roughness, Nanostructure, and  
545 Wetting on Bacterial Adhesion. *Langmuir* **2023**, *39* (15), 5426-5439. DOI:  
546 10.1021/acs.langmuir.3c00091.
- 547 (43) Bohinc, K.; Dražić, G.; Fink, R.; Oder, M.; Jevšnik, M.; Nipič, D.; Godič-Torkar, K.;  
548 Raspor, P. Available surface dictates microbial adhesion capacity. *International Journal of*  
549 *Adhesion and Adhesives* **2014**, *50*, 265-272. DOI: 10.1016/j.ijadhadh.2014.01.027.
- 550 (44) Ueshima, M.; Tanaka, S.; Nakamura, S.; Yamashita, K. Manipulation of bacterial adhesion  
551 and proliferation by surface charges of electrically polarized hydroxyapatite. *Journal of*  
552 *Biomedical Materials Research* **2002**, *60* (4), 578-584. DOI: 10.1002/jbm.10113. Yuan, Y.;  
553 Hays, M. P.; Hardwidge, P. R.; Kim, J. Surface characteristics influencing bacterial adhesion to  
554 polymeric substrates. *RSC Advances* **2017**, *7* (23), 14254-14261. DOI: 10.1039/c7ra01571b.
- 555 (45) Law, K.-Y. Definitions for Hydrophilicity, Hydrophobicity, and Superhydrophobicity:  
556 Getting the Basics Right. *The Journal of Physical Chemistry Letters* **2014**, *5* (4), 686-688. DOI:  
557 10.1021/jz402762h.
- 558 (46) Jucker, B. A.; Harms, H.; Zehnder, A. J. Adhesion of the positively charged bacterium  
559 *Stenotrophomonas (Xanthomonas) maltophilia* 70401 to glass and Teflon. *Journal of*  
560 *Bacteriology* **1996**, *178* (18), 5472-5479. DOI: 10.1128/jb.178.18.5472-5479.1996.

- 561 (47) Kreve, S.; Reis, A. C. D. Bacterial adhesion to biomaterials: What regulates this  
562 attachment? A review. *Japanese Dental Science Review* **2021**, *57*, 85-96. DOI:  
563 10.1016/j.jdsr.2021.05.003.
- 564 (48) McCaulou, D. R.; Bales, R. C.; McCarthy, J. F. Use of short-pulse experiments to study  
565 bacteria transport through porous media. *Journal of Contaminant Hydrology* **1994**, *15* (1-2), 1-  
566 14. DOI: 10.1016/0169-7722(94)90007-8.
- 567 (49) Deshpande, P. A.; Shonnard, D. R. An Improved Spectrophotometric Method To Study the  
568 Transport, Attachment, and Breakthrough of Bacteria through Porous Media. *Applied and*  
569 *Environmental Microbiology* **2000**, *66* (2), 763-768. DOI: 10.1128/aem.66.2.763-768.2000.
- 570 (50) Park, S.-J.; Lee, C.-G.; Kim, S.-B. Quantification of Bacterial Attachment-related  
571 Parameters in Porous Media. *Environmental Engineering Research* **2008**, *13* (3), 141-146. DOI:  
572 10.4491/eer.2008.13.3.141.
- 573 (51) Liu, Y.; Zhao, Q. Influence of surface energy of modified surfaces on bacterial adhesion.  
574 *Biophysical Chemistry* **2005**, *117* (1), 39-45. DOI: 10.1016/j.bpc.2005.04.015.
- 575 (52) Qi, M.; Gong, X.; Wu, B.; Zhang, G. Landing Dynamics of Swimming Bacteria on a  
576 Polymeric Surface: Effect of Surface Properties. *Langmuir* **2017**, *33* (14), 3525-3533. DOI:  
577 10.1021/acs.langmuir.7b00439.
- 578 (53) Yang, K.; Shi, J.; Wang, L.; Chen, Y.; Liang, C.; Yang, L.; Wang, L.-N. Bacterial anti-  
579 adhesion surface design: Surface patterning, roughness and wettability: A review. *Journal of*  
580 *Materials Science & Technology* **2022**, *99*, 82-100. DOI: 10.1016/j.jmst.2021.05.028.
- 581 (54) Silhavy, T. J.; Kahne, D.; Walker, S. The Bacterial Cell Envelope. *Cold Spring Harbor*  
582 *Perspectives in Biology* **2010**, *2* (5), a000414-a000414. DOI: 10.1101/cshperspect.a000414.

- 583 (55) Saha, N.; Monge, C.; Dulong, V.; Picart, C.; Glinel, K. Influence of Polyelectrolyte Film  
584 Stiffness on Bacterial Growth. *Biomacromolecules* **2013**, *14* (2), 520-528. DOI:  
585 10.1021/bm301774a.
- 586 (56) Liu, Q.; Liu, C.; Wang, S.; Zhang, L.; Sun, H.; Liao, X. Differing envelope composition of  
587 Gram-negative and Gram-positive bacteria controls the adhesion and bactericidal performance of  
588 nanoscale zero-valent iron. *Journal of Hazardous Materials* **2025**, *489*, 137663. DOI:  
589 10.1016/j.jhazmat.2025.137663.
- 590 (57) Berne, C.; Ducret, A.; Hardy, G. G.; Brun, Y. V. Adhesins Involved in Attachment to  
591 Abiotic Surfaces by Gram-Negative Bacteria. *Microbiology Spectrum* **2015**, *3* (4). DOI:  
592 10.1128/microbiolspec.mb-0018-2015.
- 593 (58) Lecuyer, S.; Rusconi, R.; Shen, Y.; Forsyth, A.; Vlamakis, H.; Kolter, R.; Stone, H. A.  
594 Shear Stress Increases the Residence Time of Adhesion of *Pseudomonas aeruginosa*. *Biophysical*  
595 *Journal* **2011**, *100* (2), 341-350. DOI: 10.1016/j.bpj.2010.11.078.
- 596 (59) Tufenkji, N. Modeling microbial transport in porous media: Traditional approaches and  
597 recent developments. *Advances in Water Resources* **2007**, *30* (6-7), 1455-1469. DOI:  
598 10.1016/j.advwatres.2006.05.014.
- 599